View metadata, citation and similar papers at core.ac.uk

brought to you by CORE

Influence of alloying elements Ni and Nb on thermal stability and corrosion resistance of Cu-based bulk metallic glasses

C.L. Qin[a)]
Japan Science and Technology Agency, Institute for Materials Research, Tohoku University, Aoba-ku, Sendai 980-8577, Japan

W. Zhang, K. Asami, H. Kimura, and A. Inoue
Institute for Materials Research, Tohoku University, Sendai 980-8577, Japan

(Received 9 January 2007; accepted 9 March 2007)

Bulk metallic glasses (BMGs) with critical diameters of 2.5–3 mm were synthesized in the $(Cu_{0.6}Zr_{0.3}Ti_{0.1})_{100-x-y}Ni_yNb_x$ system by copper-mold casting. These alloys exhibit a large supercooled liquid region (ΔT_x) of 40–60 K and a high reduced glass transition temperature (T_g/T_l) of 0.60–0.61, indicating high glass-forming ability and high thermal stability of the supercooled liquid. The corrosion rates in 1 N HCl and 3 mass% NaCl solutions significantly decrease by simultaneous alloying with Ni and Nb elements. The addition is also effective in raising the pitting potential in chloride solutions. The addition of Ni and Nb is favorable for the alloys in forming Zr-, Ti-, and Nb-enriched highly protective surface films in HCl and NaCl solutions.

I. INTRODUCTION

A great deal of research has been carried out on recently developed Cu-based bulk metallic glasses (BMGs), as exemplified for the Cu–(Zr,Hf)–Ti,[1–3] Cu–(Zr,Hf)–Al,[4–7] Cu–Zr–Al–(Ti,Y),[8,9] Cu–Zr–Ti–Ag[10] systems. The Cu-based BMGs are known for their ultrahigh strength exceeding 2 GPa, high glass-forming ability (GFA), and good wear resistance; they have potential applications as advanced engineering materials in many areas, such as surgical instruments and bipolar plates in fuel cells. In particular, Cu–Zr–Ti-based BMGs, with low-cost fabrication and easy forming ability in the viscous state, show high potential for application. However, the corrosion resistance of these Cu-based BMGs is not always better than that for conventional Cu-based crystalline alloys, though the tensile strength levels are 2 to 5 times higher for the Cu-based BMGs.[11] Therefore, there is a need to improve their corrosion resistance to make them acceptable for use on the industrial level. In our previous work, the effects of different alloying elements on thermal stability, GFA, and corrosion resistance of Cu–Zr(Hf)–Ti-based BMGs were investigated.[12–15] The addition of Mo, Ta, or Nb effectively improves the corrosion resistance of the Cu–Zr(Hf)–Ti-based BMGs in various aggressive environments. Unfortunately, the supercooled liquid region (ΔT_x) decreases greatly with alloying additional elements, resulting in a decrease in GFA and thermal stability of the supercooled liquid before crystallization. Therefore, the limitations of thermal stability and composition range for the glass formation for the Cu–Zr(Hf)–Ti-based alloys will prevent further extension of their applications. Great efforts have been devoted to developing new BMGs with larger supercooled liquid region and good viscous flow workability in conjunction with higher corrosion resistance.

Recently, we found that the addition of 5 at.% Ni to Cu–Zr(Hf)–Ti-based BMGs caused a significant increase in the supercooled liquid region and the extension of the composition range for the bulk metallic glass formation. In addition, the simultaneous addition of Ni and Nb elements is effective for the improvement of corrosion resistance in the maintenance of high GFA. The present study aimed to investigate the effects of additional elements Ni and Nb on thermal properties, GFA, and corrosion resistance of Cu–Zr–Ti–Ni–Nb alloys. X-ray photoelectron spectroscopy (XPS) analysis was performed to clarify the surface-related chemical characteristics of the alloy before and after immersion in the solutions; this has led to better understanding of the correlation between the surface composition and the corrosion resistance.

II. EXPERIMENTAL PROCEDURE

Master alloys with nominal compositions of $(Cu_{0.6}Zr_{0.3}Ti_{0.1})_{100-x-y}Ni_yNb_x$ (x = 0 to 6 at.% and y = 0 to 7 at.%) were prepared from pure elemental Cu, Zr, Ti, Ni, and Nb of 99.9 mass% purity by arc melting under an argon atmosphere using a water-cooled Cu hearth. At

[a)]Address all correspondence to this author.
e-mail: clqin@imr.tohoku.ac.jp
DOI: 10.1557/JMR.2007.0206

 © 2007 Materials Research Society

first, the binary alloy of Zr and Nb was prepared. This binary alloy was then melted with Cu, Ti, and Ni. Remelted ingots were ejected into a copper mold to produce a 50-mm-long cylindrical rod with diameters up to 4 mm. The structure of the specimens was examined by x-ray diffraction (XRD) using Cu K_α radiation. The thermal stability associated with glass transition temperature (T_g) and crystallization temperature (T_x) for the glassy alloys was investigated by differential scanning calorimetry (DSC) at a heating rate of 0.67 K/s. The liquidus temperature was determined by differential thermal analysis (DTA) at a heating and cooling rate of 0.033 K/s.

The corrosion behavior of the BMGs was evaluated by weight loss and electrochemical measurements. The specimens were 2 cm long with a diameter of 1.5 mm. Prior to corrosion tests, the specimens were mechanically polished in cyclohexane with silicon carbide paper up to grit 2000, degreased in acetone, washed in distilled water, dried in air, and further exposed to air for 24 h for good reproducibility. Electrolytes of 1 N HCl and 3 mass% NaCl solutions open to air were used at room temperature (about 298 K). The solutions were prepared from reagent grade chemicals and high-purity deionized water. The corrosion rates were estimated from the weight loss after immersion in the solutions for 1 week. The weight loss for each alloy was measured three times, and the average value was used for estimation of the corrosion rate. Electrochemical measurements were conducted in a three-electrode cell using a platinum counter electrode and an Ag/AgCl reference electrode. Potentiodynamic polarization curves were measured at a potential sweep rate of 50 mV min^{-1} after open-circuit immersion for about 20 min when the open-circuit potential became almost steady.

XPS measurements for surface analysis of the specimens before and after immersion in the solutions were performed using an SSI SSX-100 photoelectron spectrometer (Surface Science, Inc., US) with monochromatized Al K_α excitation ($h\nu = 1486.6$ eV). The composition of the surface film and the composition of the underlying alloy surface were quantitatively determined with a previously proposed method using the integrated intensities of photoelectrons under the assumption of a three-layer model of an outmost contaminant hydrocarbon layer of uniform thickness, a surface film of uniform thickness, and an underlying alloy surface of infinite thickness with regard to x-ray photoelectrons.[16,17]

III. RESULTS AND DISCUSSION

A. Effects of Ni and Nb additions on the GFA and thermal stability

From XRD patterns in Fig. 1, it can be seen that bulk alloys with a diameter of 1.5 mm consisting of a glassy

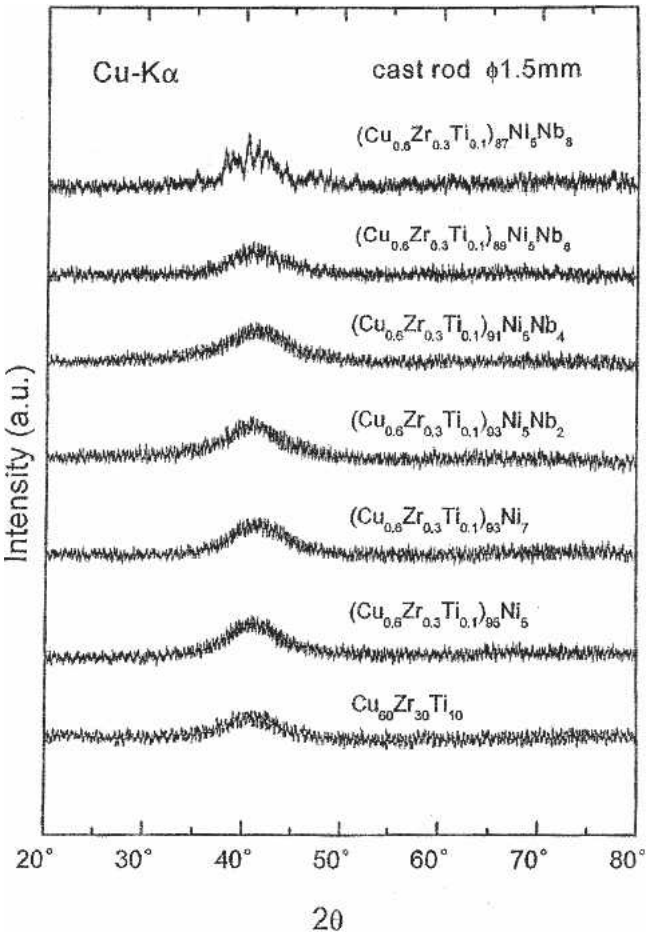

FIG.1. XRD patterns of the as-cast $(Cu_{0.6}Zr_{0.3}Ti_{0.1})_{100-x-y}Ni_yNb_x$ rods with a diameter of 1.5 mm.

single phase without crystallinity were fabricated in a wide composition range of 0–7 at.% Ni and 0–6 at.% Nb for the $(Cu_{0.6}Zr_{0.3}Ti_{0.1})_{100-x-y}Ni_yNb_x$ alloys. Figure 2 shows DSC curves of the $(Cu_{0.6}Zr_{0.3}Ti_{0.1})_{100-x}Ni_x$ BMG rods with a diameter of 1.5 mm, where T_g and T_x correspond to glass transition temperature and onset temperature of crystallization, respectively. By addition of Ni element, the supercooled liquid region ($\Delta T_x = T_x - T_g$) significantly increases from 40 K at 0 at.% Ni to 60 K at 5 at.% Ni and then decreases to 56 K at 7 at.% Ni, accompanied by the change in the crystallization mode from multiple stages to a single stage. The critical diameter for glass formation (d_c) was 3 mm at 5 at.% Ni and 2.5 mm at 7 at.% Ni. As a result, the $(Cu_{0.6}Zr_{0.3}Ti_{0.1})_{95}Ni_5$ quaternary alloy is the optimum in the GFA and thermal stability of the supercooled liquid region. With the further addition of Nb to the $(Cu_{0.6}Zr_{0.3}Ti_{0.1})_{95}Ni_5$ quaternary alloy, the DSC curves of the as-cast 1.5 mm $(Cu_{0.6}Zr_{0.3}Ti_{0.1})_{100-x-y}Ni_yNb_x$ glassy rods are shown in Fig. 3. As the Nb content increases, the T_g increases slightly while the T_x decreases, resulting in a decrease in ΔT_x from 60 K at 0 at.% Nb to 40 K at 6 at.% Nb. The

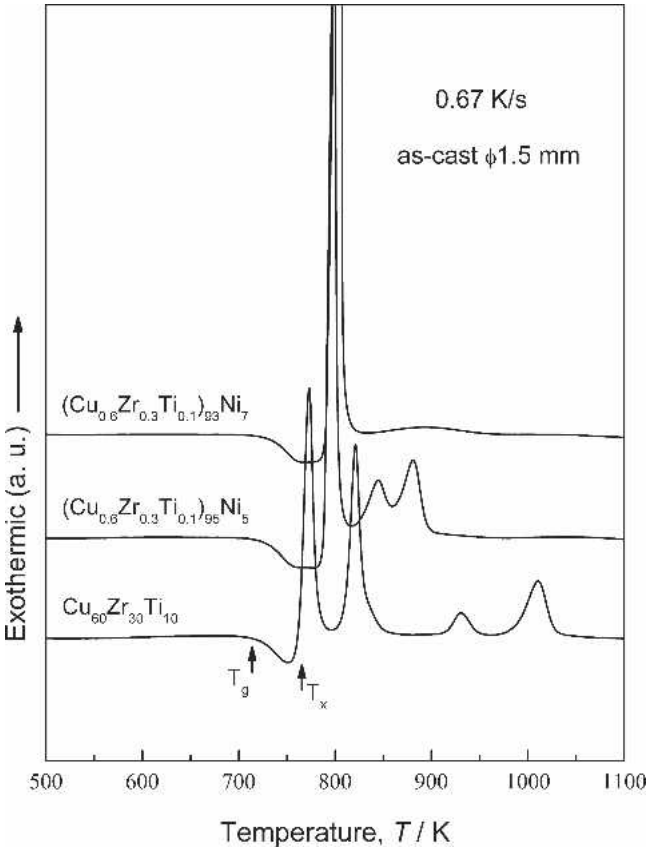

FIG. 2. DSC curves of the as-cast $(Cu_{0.6}Zr_{0.3}Ti_{0.1})_{100-x}Ni_x$ (x = 0 to 7 at.%) glassy rods with a diameter of 1.5 mm.

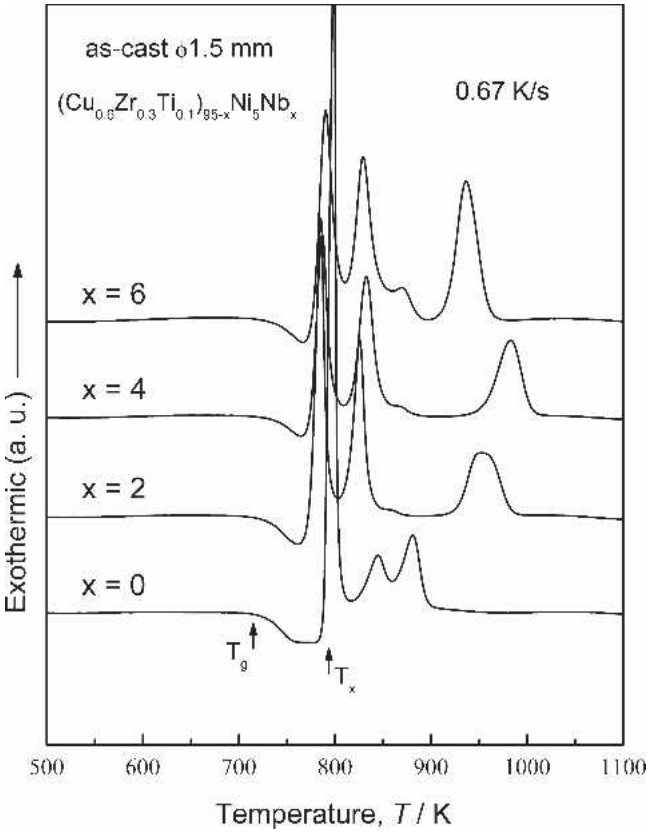

FIG. 3. DSC curves of the as-cast $(Cu_{0.6}Zr_{0.3}Ti_{0.1})_{95-x}Ni_5Nb_x$ (x = 0 to 6 at.%) glassy rods with a diameter of 1.5 mm.

critical diameter was 3 mm for the alloys with Nb contents up to 4 at.% and 2.5 mm for the 6 at.% Nb alloy. The results indicate that the Cu–Zr–Ti–Ni–Nb alloys still keep rather high GFA, although the additional element Nb shows negative effect on the GFA and thermal stability. Based on these DSC curves in Figs. 2 and 3, the composition dependence of T_g, T_x, ΔT_x, and d_c for the $(Cu_{0.6}Zr_{0.3}Ti_{0.1})_{100-x-y}Ni_yNb_x$ BMGs is summarized in Table I. It is seen that the ΔT_x shows a maximum value of 60 K at $(Cu_{0.6}Zr_{0.3}Ti_{0.1})_{95}Ni_5$ and decreases with increasing Nb content. Accordingly, the Cu-based BMGs with alloying elements Ni and Nb possess the critical diameters of 2.5–3 mm and large ΔT_x values of 40–60 K in the Cu–Zr–Ti–Ni–Nb system, indicating the high GFA and high thermal stability.

To investigate the reason for the high GFA in the wide composition range for the present alloys, liquidus temperature (T_l) values were measured by DTA at a cooling rate of 0.033 K/s, as shown in Fig. 4. T_l increases with increasing Ni content and slightly increases with further addition of Nb to the $(Cu_{0.6}Zr_{0.3}Ti_{0.1})_{95}Ni_5$ alloy. According to the T_g values obtained by DSC and the T_l values obtained by DTA for the alloys, the reduced glass transition temperature (T_g/T_l) values are evaluated to be in the range of 0.60 to 0.61, as shown in Table I. The rather high T_g/T_l values of the Cu–Zr–Ti–Ni–Nb alloy system are consistent with the formation of bulk metallic glasses with critical diameters of 2.5–3 mm in the wide composition range, although the T_g/T_l value decreases with increasing Ni and Nb contents.

It has been reported that the high GFA leading to the formation of a bulk metallic glass is obtained in the multicomponent alloy systems according to the following three empirical rules[18–20]: (i) multicomponent system consisting of more than three elements, (ii) significant atomic size mismatches above 12%, and (iii) suitable negative heats of mixing. As reported in the Cu–Zr(Hf)–Ti–Nb alloys,[13–15] additional Nb element has nearly zero

TABLE I. Thermal properties and critical diameters (d_c) of glassy alloys.

Alloy	T_g (K)	T_x (K)	ΔT_x (K)	T_l (K)	T_g/T_l	d_c (mm)
$Cu_{60}Zr_{30}Ti_{10}$	719	759	40	1170	0.61	4.0
$(Cu_{0.6}Zr_{0.3}Ti_{0.1})_{95}Ni_5$	727	787	60	1198	0.61	3.0
$(Cu_{0.6}Zr_{0.3}Ti_{0.1})_{93}Ni_7$	735	791	56	1225	0.60	2.5
$(Cu_{0.6}Zr_{0.3}Ti_{0.1})_{93}Ni_5Nb_2$	728	778	50	1204	0.61	3.0
$(Cu_{0.6}Zr_{0.3}Ti_{0.1})_{91}Ni_5Nb_4$	730	776	46	1209	0.60	3.0
$(Cu_{0.6}Zr_{0.3}Ti_{0.1})_{89}Ni_5Nb_6$	735	775	40	1214	0.60	2.5

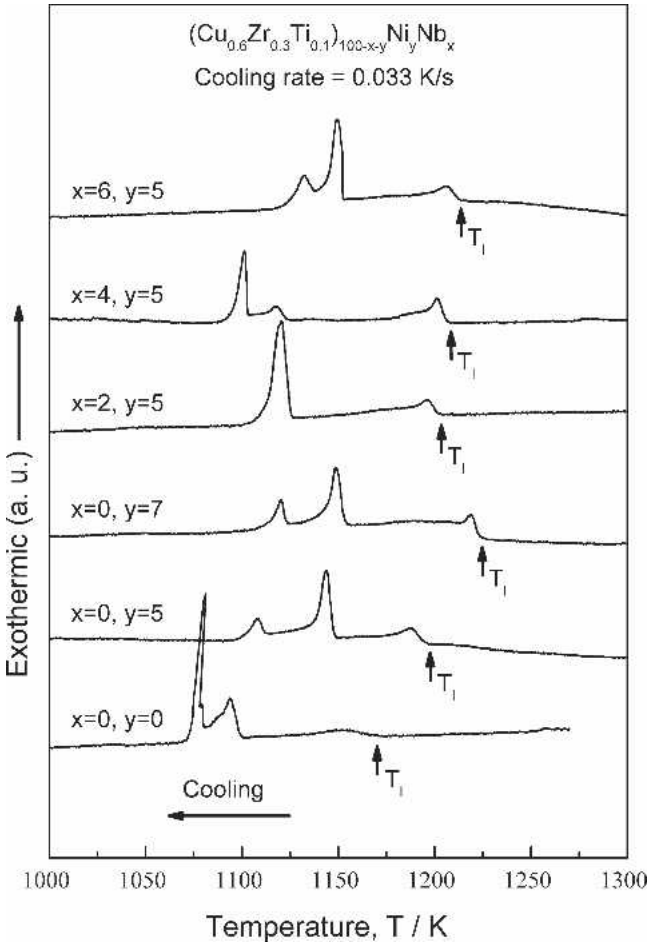

FIG. 4. DTA curves of the $(Cu_{0.6}Zr_{0.3}Ti_{0.1})_{100-x-y}Ni_yNb_x$ ($x = 0$ to 6 at.% and $y = 0$ to 7 at.%) alloys.

or positive heat of mixing against the base constituent elements of Cu, Zr(Hf), and Ti. The effect of addition of Nb shows a deviation from the third of the empirical rules. However, for the present Cu–Zr–Ti–Ni–Nb alloys, the atomic size of Ni is 0.125 nm, and hence the addition of Ni gives rise to the following sequent change in their atomic sizes, i.e., Zr(0.162 nm) > Ti(0.147 nm) > Nb(0.143 nm) > Cu (0.128 nm) > Ni (0.125 nm).[21] Because of the smallest atomic radius of Ni among the constituent elements, it is suggested that Ni is likely to infill a vacant site among the atoms in the disordered structure, leading to the release of extra free energy and the increase in the stability of a glassy state. On the other hand, Ni has highly negative heats of mixing with Zr, Ti, and Nb of –49, –35, and –30 kJ/mol,[22] respectively. These values are even larger than those for Cu–Zr and Cu–Ti atomic pairs of –23 and –9 kJ/mol, respectively. As a result, atomic size effect among the constituents and the strong chemical affinities of Ni–Zr, Ni–Ti, and Ni–Nb cause an increase in the degree of the satisfaction of the three empirical rules, which leads to the formation of a new liquid structure with highly dense random packed atomic configurations, new local atomic configurations, and long-range homogeneous atomic configurations with strong interaction.[18–20] The increase and maintenance of the bulk glass-forming ability in the wide Nb content range for the Cu–Zr–Ti–Ni–Nb alloys is due to the existence of Ni element. Meanwhile, the strong Ni–Nb bonding pair also supports the present result.

B. Effects of Ni and Nb additions on corrosion resistance

Figures 5 and 6 show the average corrosion rates of the as-cast 1.5 mm $(Cu_{0.6}Zr_{0.3}Ti_{0.1})_{100-x-y}Ni_yNb_x$ glassy rods immersed in 1 N HCl and 3 mass% NaCl solutions at 298 K open to air for 1 week, respectively. The corrosion rates of the alloys containing only Nb and an industrial brass (60 wt% Cu + 40 wt% Zn) are also presented for comparison. In Fig. 5, the corrosion rate in 1 N HCl is 0.66 mm/year for $Cu_{60}Zr_{30}Ti_{10}$. The corrosion rate decreases significantly to about 0.1–0.2 mm/year by the addition of 5–7 at.% Ni or 2–4 at.% Nb and further decreases by the simultaneous addition of Ni and Nb. No weight loss is detected for the $(Cu_{0.6}Zr_{0.3}Ti_{0.1})_{89}Ni_5Nb_6$ glassy alloy, indicating a corrosion rate of less than 1×10^{-3} mm/year, which was the detection limit for the present measurement. It is, therefore, evident that the simultaneous addition of Ni and Nb to the alloys is more effective for improving the corrosion resistance in the strong corrosive solution. Similar remarkable improvement of corrosion rate is also recognized in 3 mass% NaCl solution, as shown in Fig. 6. The addition of 5 at.% Ni or 5 at.% Nb causes a significant decrease in corrosion rate from 0.29 mm/year for $Cu_{60}Zr_{30}Ti_{10}$ to 0.013 or 0.018 mm/year, respectively. No appreciable loss in sample weight is detected for the alloys simultaneously

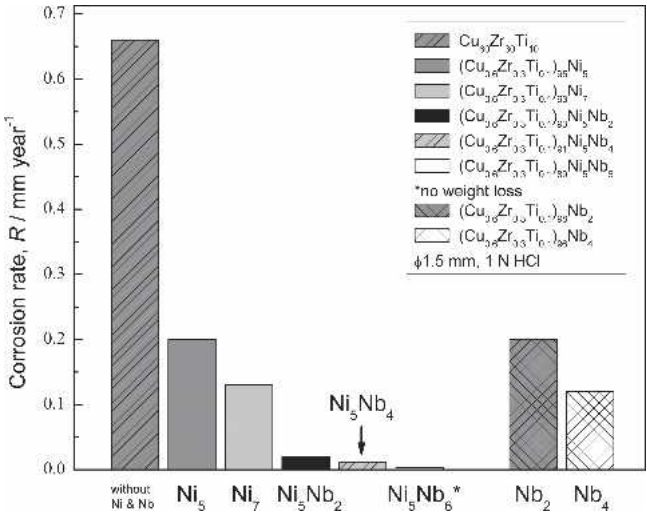

FIG. 5. Corrosion rates of the Cu–Zr–Ti–Ni–Nb BMGs in 1 N HCl solution at 298 K open to air.

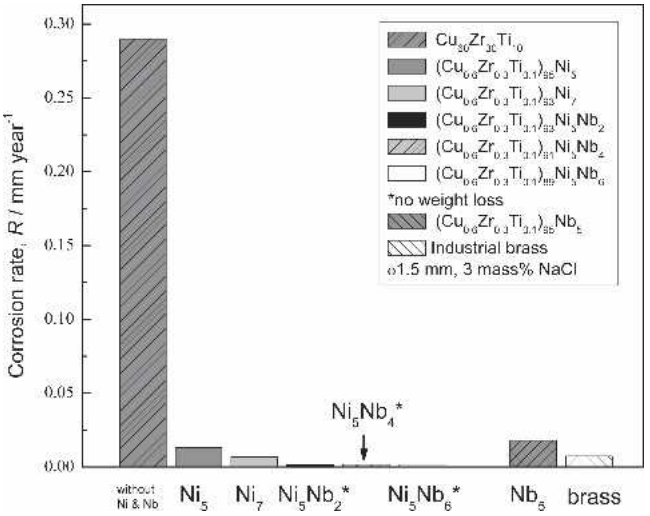

FIG. 6. Corrosion rates of the Cu–Zr–Ti–Ni–Nb BMGs and an industrial brass in 3 mass% NaCl solution at 298 K open to air.

containing Ni and Nb elements. Furthermore, it is well-known that the industrial brass exhibits high corrosion resistance in sea water. The corrosion resistance of the 7 at.% Ni alloy is almost the same as that of the industrial brass, and the corrosion resistance of the alloys by the simultaneous addition of Ni and Nb elements is better than that of the industrial brass. Therefore, the Cu-based BMGs with simultaneously alloying Ni and Nb elements exhibit high corrosion resistance under strong corrosion conditions, resulting from the synergistic effect of Ni and Nb additions.

Figure 7 shows anodic polarization curves for the as-cast 1.5 mm $(Cu_{0.6}Zr_{0.3}Ti_{0.1})_{100-x-y}Ni_yNb_x$ glassy alloys in 3 mass% NaCl solution at 298 K. It is clearly seen that the alloys with and without Ni exhibit different polarization behavior. The alloys without Ni suffer general corrosion. However, the alloys containing Ni are spontaneously passivated with low passive current density, although they suffer pitting corrosion by anodic polarization. Moreover, their pitting corrosion potentials are nobler with an increase in Ni and Nb contents. In particular, the simultaneous addition of Ni and Nb to the alloys is beneficial for enhancing the pitting corrosion potential against localized corrosion in chloride-containing solutions.

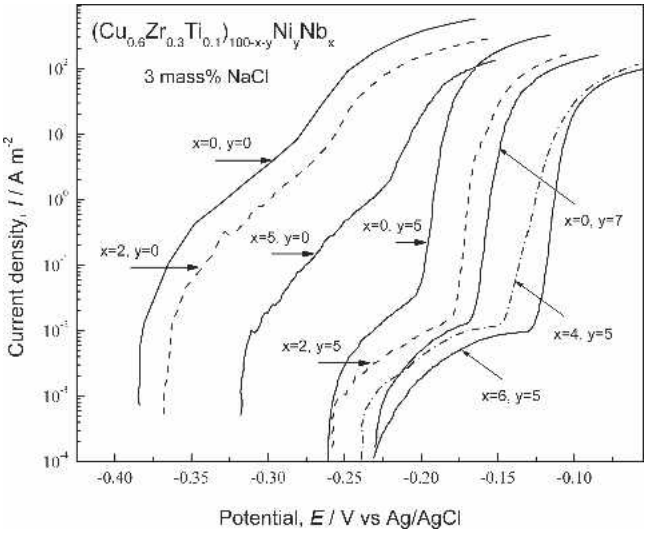

FIG. 7. Anodic polarization curves of the Cu–Zr–Ti–Ni–Nb BMGs in 3 mass% NaCl solutions at 298 K.

C. XPS analysis of surface film

To clarify the synergistic effect of alloying elements Ni and Nb on the corrosion resistance and the surface-related chemical characteristics of the alloys, XPS analysis was performed for the $(Cu_{0.6}Zr_{0.3}Ti_{0.1})_{89}Ni_5Nb_6$ alloy as-polished mechanically in cyclohexane or immersed for one week in 1 N HCl and 3 mass% NaCl solutions. The XPS spectra of the specimens over a wide binding energy region exhibited peaks of Cu 2*p*, Zr 3*d*, Ti 2*p*, Ni 2*p*, Nb 3*d*, O 1*s*, and C 1*s*. The C 1*s* spectrum showing a peak at around 285.0 eV arose from a contaminant hydrocarbon layer covering the topmost surface of the specimen. The O 1*s* spectrum was composed of at least two overlapping peaks, which were so-called OM and OH oxygen. The OM oxygen corresponds to O^{2-} ions in oxyhydroxide and/or oxide, and the OH oxygen is oxygen linked to proton in the film, composed of OH^- ions and bound water in the surface film.[16,23] The photoelectron spectrum of Cl arising from the solution species was less than the detectable level. The spectrum peaks from alloy constituents were composed of peaks of oxidized states and metallic states; the oxidized states (ox) and metallic states (m) are assigned to signals from the surface film and underlying alloy surface just beneath the surface film, respectively. However, on the other specimens, those peaks showed only oxidic peaks because the surface films on the specimens were much thicker than the escape depths of photoelectrons. Considering the Cu 2*p* electron spectrum and the Cu $L_3M_{4,5}M_{4,5}$ Auger peaks, the copper was distinguished as Cu^{2+}, Cu^+, and Cu^0 states.

Figure 8 shows examples of the deconvolution of (a) Zr 3*d* spectrum for the alloy exposed to air after mechanical polishing and (b) Ti 2*p* spectrum of the alloy immersed in 3 mass% NaCl at 298 K for 168 h. In Fig. 8(a), the Zr $3d_{5/2}$ and Zr $3d_{3/2}$ peaks consist of two doublets: the Zr $3d_{5/2}$ and $3d_{3/2}$ peaks corresponding to the metallic state Zr^0 are located at 179.4 and 181.5 eV, respectively, and those corresponding to the Zr^{4+} state appear at 182.7 and 185.1 eV, respectively. The Ti 2*p* spectrum [Fig. 8(b)] consists of one set of $2p_{3/2}$ and $2p_{1/2}$ peaks of oxidized state. The peaks located at 458.8 and 464.5 eV are assigned to Ti 2*p* electrons of Ti^{4+} ions. No peak corresponding to metallic state (Ti^0) was detected.

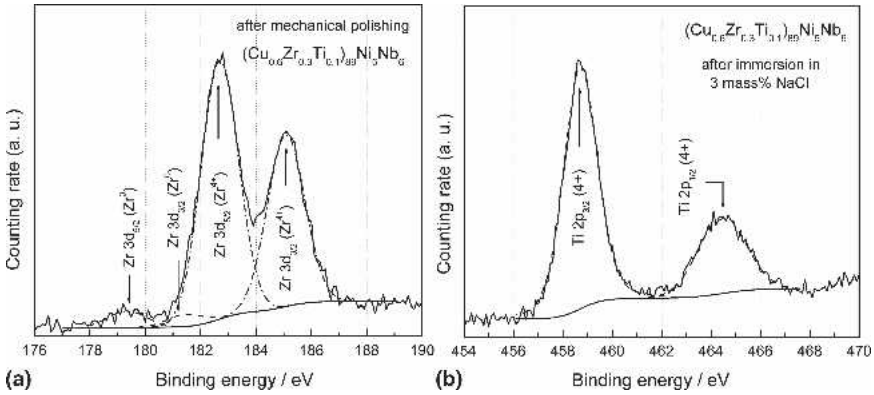

FIG. 8. Example of deconvolution of (a) Zr 3*d* spectrum for $(Cu_{0.6}Zr_{0.3}Ti_{0.1})_{89}Ni_5Nb_6$ alloy exposed to air and (b) Ti 2*p* spectrum measured for the alloy after immersion in 3 mass% NaCl solution at 298 K for 1 week.

Figure 9 shows an example of deconvolution of the Cu $2p_{3/2}$ peaks and Cu^{2+} satellite peaks obtained from the alloy exposed to air after mechanical polishing. The Cu^0 and Cu^+ peaks overlap each other. By analysis and deconvolution of the Cu $L_3M_{4,5}M_{4,5}$ Auger peaks, the copper was separated as Cu^{2+}, Cu^+, and Cu^0 states.

After integrated intensities of the peaks for individual species were obtained, the thickness and composition of the surface film and the composition of the underlying alloy surface were determined quantitatively using a previously proposed method.[16,17] Figure 10 shows the surface film compositions of the $(Cu_{0.6}Zr_{0.3}Ti_{0.1})_{89}Ni_5Nb_6$ alloy exposed to air and those immersed in the 1 N HCl and 3 mass% NaCl solutions after mechanical polishing. In the surface film formed by air exposure after mechanical polishing, the ratio of the fractions of Cu, Zr, Ti, Ni, and Nb is about 45.5:32.5:14.7:2.1:5.2 (the nominal ratio Cu:Zr:Ti:Ni:Nb = 53.4:26.7:8.9:5:6). The cationic fractions of Zr and Ti increase in the surface film, whereas those of Cu, Ni, and Nb cations reduce with respect to the alloy composition. This fact indicates that the preferential oxidation of Zr and Ti occurs in the air-formed film. Consequently, air exposure of $(Cu_{0.6}Zr_{0.3}Ti_{0.1})_{89}Ni_5Nb_6$ alloy after mechanical polishing results in preferential oxidation of Ti and Zr in the surface, and deficiency of Cu, Ni, and Nb elements in the surface. The major cations in the surface film were Cu^{2+}, Cu^+, Zr^{4+}, Ti^{4+}, Ni^{2+}, and Nb^{5+}.

Immersion for 168 h in different solutions gives rise to the formation of a new film, which is different from the air-formed film. When the alloy is immersed in HCl solution, the fraction of Cu cations in the surface film significantly decreases as compared with that in air-formed

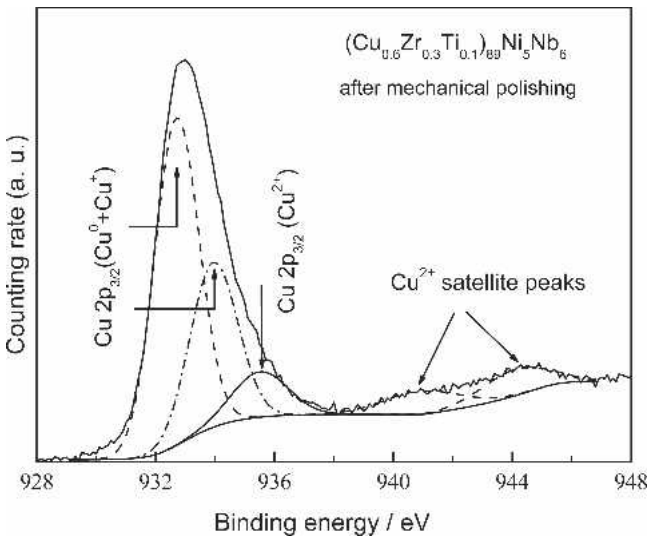

FIG. 9. Cu 2*p* spectrum for $(Cu_{0.6}Zr_{0.3}Ti_{0.1})_{89}Ni_5Nb_6$ alloy exposed to air after mechanical polishing.

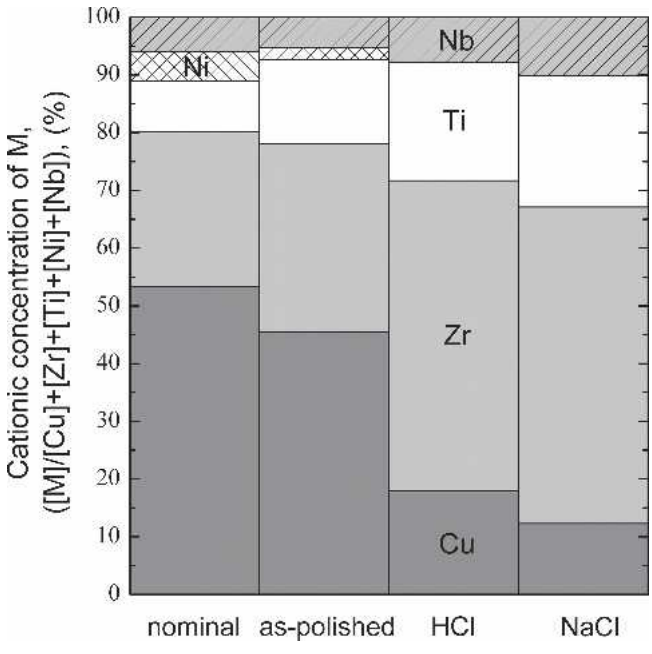

FIG. 10. Changes in cationic fractions in the surface film for the as-cast $(Cu_{0.6}Zr_{0.3}Ti_{0.1})_{89}Ni_5Nb_6$ alloy exposed to air and samples immersed in 1 N HCl, 3 mass% NaCl solutions open to air for 1 week after mechanical polishing.

surface and reduces more after immersion in the 3 mass% NaCl solution. Simultaneously, the cationic fractions of Zr and Ti cations greatly increase in the alloy surface immersed in the HCl and NaCl solutions. On the other hand, it is found that the surface films of the alloy immersed in the solutions are enriched in Nb with respect to that in the as-polished film or the alloy Nb content. It is worth noting that no Ni element is observed in the surface film after immersion in those solutions, implying rapid initial preferential dissolution of Ni in the surface film.[24–26] Therefore, open-circuit immersion leads to the formation of Zr-, Ti-, and Nb-enriched surface film as a result of rapid initial preferential dissolution of Cu and Ni.

The nature of passive surface films on the alloys plays a vital role in the mechanism of corrosion resistance. Generally, the passivation of alloys occurs through the active dissolution of metals at the initial periods of immersion in a solution. The high chemical reactivity of the alloys brings on the rapid accumulation of beneficial species in the passive film. In Fig. 7, it is clearly seen that the Cu–Zr–Ti–Ni–Nb alloys with and without Ni exhibit different polarization behavior in 3 mass% NaCl solution. The alloys containing Ni are spontaneously passivated with low passive current density. The XPS results shown in Fig. 10, provide clarification that open-circuit immersion in HCl and NaCl solutions for the $(Cu_{0.6}Zr_{0.3}Ti_{0.1})_{89}Ni_5Nb_6$ alloy leads to the rapid accumulation of the beneficial species Zr, Ti, and Nb cations in higher concentration at the alloy/solution interface after the initial fast dissolution of the active components Cu and Ni, and hence spontaneous passivation occurs. After passivation, the passive films, which are highly enriched in Zr, Ti, and Nb cations and largely deficient in Cu cations, are protective enough to prevent further dissolution of Cu and Ni through the surface. As indicated by the results of immersion testing, when the present alloy was immersed in those solutions for 1 week, no weight loss was detected with the present microbalance. This in turn verifies the high stability of the passive states. Therefore, it is considered that the addition of Ni helps to enhance the accumulation of beneficial passivating elements (Zr, Ti, and Nb) on the alloy surface as a result of fast dissolution of alloy constituents (Cu and Ni), resulting in the formation of a highly protective passive film in comparison with the alloys free of Ni. In return, the enrichment of Nb element in the surface film provides a high passivating ability for the present alloy immersed in those solutions. Comparing the alloys without Ni and Nb, i.e., $Cu_{60}Zr_{30}Ti_{10}$ and $(Cu_{0.6}Zr_{0.3}Ti_{0.1})_{95}Nb_5$,[13] the Cu content was largely concentrated in the surface films of the $Cu_{60}Zr_{30}Ti_{10}$ alloy after immersion in HCl and NaCl solutions. The surface film containing such a large amount of Cu could not protect the alloy against corrosion.[13,15,27] Although the addition of 5 at.% Nb to Cu–Zr–Ti alloy decreased the Cu content in the surface and modified the surface film of the $(Cu_{0.6}Zr_{0.3}Ti_{0.1})_{95}Nb_5$ immersed in the corrosive solutions, the Cu concentration in the surface was still high. It can, therefore, be said that the protective quality of the surface films is improved by the presence of Ni and Nb. Consequently, the origin of high corrosion resistance for the present alloy in chloride containing solutions is explained by formation of the highly protective Zr-, Ti-, and Nb-enriched surface film, which is able to separate the bulk of the alloy from the corrosive solutions.

IV. CONCLUSIONS

The synergistic influence of Ni and Nb elements on the glass-forming ability, thermal stability of supercooled liquid, and corrosion resistance of $(Cu_{0.6}Zr_{0.3}Ti_{0.1})_{100-x-y}Ni_yNb_x$ alloys was investigated. The results are summarized as follows:

(1) The addition of Ni element causes an extension of a supercooled liquid region from 40 K for $Cu_{60}Zr_{30}Ti_{10}$ to 60 K for $(Cu_{0.6}Zr_{0.3}Ti_{0.1})_{95}Ni_5$, which is effective for the increase in thermal stability of the supercooled liquid before crystallization.

(2) The $(Cu_{0.6}Zr_{0.3}Ti_{0.1})_{100-x-y}Ni_yNb_x$ ($x = 0$ to 6 at.% and $y = 0$ to 7 at.%) alloys can be synthesized in a bulk glassy form with critical diameters of 2.5–3 mm by copper-mold casting, although the GFA and thermal stability exhibit a slight decrease with the addition of Nb element.

(3) The simultaneous addition of Ni and Nb to the Cu–Zr–Ti alloys is effective for improving synergistically the corrosion resistance of the alloys by remarkably decreasing the corrosion rates in chloride containing solutions and enhancing the pitting potential against the localized corrosion.

(4) The highly protective Zr-, Ti-, and Nb-enriched surface film is formed by the rapid initial preferential dissolution of Cu and Ni, which is able to separate the bulk of the alloy from the corrosive solutions.

ACKNOWLEDGMENT

The authors acknowledge Mr. N. Ohtsu for helping with XPS measurements.

REFERENCES

1. A. Inoue, W. Zhang, T. Zhang, and K. Kurosaka: High-strength Cu-based bulk glassy alloys in Cu–Zr–Ti and Cu–Hf–Ti ternary systems. *Acta Mater.* **49,** 2645 (2001).
2. A. Inoue, W. Zhang, T. Zhang, and K. Kurosaka: Formation and mechanical properties of Cu–Hf–Ti bulk glassy alloys. *J. Mater. Res.* **16,** 2836 (2001).
3. Q. Cao, J. Li, Y. Zhou, and J.Z. Jiang: Mechanically driven phase separation and corresponding microhardness change in

$Cu_{60}Zr_{20}Ti_{20}$ bulk metallic glass. *Appl. Phys. Lett.* **86,** 081913 (2005).
4. A. Inoue and W. Zhang: Formation, thermal stability and mechanical properties of Cu–Zr–Al bulk glassy alloys. *Mater. Trans.* **43,** 2921 (2002).
5. A. Inoue and W. Zhang: Formation and mechanical properties of Cu–Hf–Al bulk glassy alloys with a large supercooled liquid region of over 90 K. *J. Mater. Res.* **18,** 1435 (2003).
6. J. Das, M.B. Tang, K.B. Kim, R. Theissmann, F. Baier, W.H. Wang, and J. Eckert: "Work-hardenable" ductile bulk metallic glass. *Phys. Rev. Lett.* **94,** 205501 (2005).
7. K.B. Kim, J. Das, F. Baier, M.B. Tang, W.H. Wang, and J. Eckert: Heterogeneity of a $Cu_{47.5}Zr_{47.5}Al_5$ bulk metallic glass. *Appl. Phys. Lett.* **88,** 051911 (2006).
8. H. Men, W.T. Kim, and D.H. Kim: Effect of titanium on glass-forming ability of Cu–Zr–Al alloys. *Mater. Trans.* **44,** 1647 (2003).
9. D.H. Xu, G. Duan, and W.L. Johnson: Unusual glass-forming ability of bulk amorphous alloys based on ordinary metal copper. *Phys. Rev. Lett.* **92,** 245504 (2004).
10. C.L. Dai, H. Guo, Y. Shen, Y. Li, E. Ma, and J. Xu: A new centimeter-diameter Cu-based bulk metallic glass. *Scripta Mater.* **54,** 1403 (2006).
11. *Annual Book of ASTM Standards* (ASTM, West Conshohocken, PA, 1997), p. 773.
12. K. Asami, C.L. Qin, T. Zhang, and A. Inoue: Effect of additional elements on the corrosion behavior of a Cu–Zr–Ti bulk metallic glass. *Mater. Sci. Eng., A* **375–377,** 235 (2004).
13. C.L. Qin, K. Asami, T. Zhang, W. Zhang, and A. Inoue: Corrosion behavior of Cu–Zr–Ti–Nb bulk glassy alloys. *Mater. Trans.* **44,** 749 (2003).
14. C.L. Qin, K. Asami, T. Zhang, W. Zhang, and A. Inoue: Effects of additional elements on the glass formation and corrosion behavior of bulk glassy Cu–Hf–Ti alloys. *Mater. Trans.* **44,** 1042 (2003).
15. C.L. Qin, W. Zhang, K. Asami, N. Ohtsu, and A. Inoue: Glass formation, corrosion behavior and mechanical properties of bulk glassy Cu–Hf–Ti–Nb alloys. *Acta Mater.* **53,** 3903 (2005).
16. K. Asami, K. Hashimoto, and S. Shimodaira: XPS determination of compositions of alloy surfaces and surface oxides on mechanically polished iron-chromium alloys. *Corros. Sci.* **17,** 713 (1977).
17. K. Asami and K. Hashimoto: An XPS study of the surfaces on Fe–Cr, Fe–Co and Fe–Ni alloys after mechanical polishing. *Corros. Sci.* **24,** 83 (1984).
18. A. Inoue: Stabilization of metallic supercooled liquid and bulk amorphous alloys. *Acta Mater.* **48,** 279 (2000).
19. A. Inoue: Bulk amorphous alloys with soft and hard magnetic properties. *Mater. Sci. Eng., A* **226–228,** 357 (1997).
20. A. Inoue: High strength bulk amorphous alloys with low critical cooling rates. *Mater. Trans., JIM* **36,** 866 (1995).
21. *Metals Databook,* edited by Japan Institute of Metals (Maruzen, Tokyo, Japan, 1983), p. 8.
22. F.R. Boer, R. Boom, W.C.M. Mattens, A.R. Miedema, and A.K. Niessen: *Cohesion in metals* (North-Holland, Amsterdam, The Netherlands, 1988), p. 224.
23. K. Asami and K. Hashimoto: The x-ray photo-electron spectra of several oxides of iron and chromium. *Corros. Sci.* **17,** 559 (1977).
24. H.J. Lee, E. Akiyama, H. Habazaki, A. Kawashima, K. Asami, and K. Hashimoto: The roles of tantalum and phosphorus in the corrosion behavior of Ni–Ta–P alloys in 12 M HCl. *Corros. Sci.* **39,** 321 (1997).
25. H. Katagiri, S. Meguro, M. Yamasaki, H. Habazaki, T. Sato, A. Kawashima, K. Asami, and K. Hashimoto: Synergistic effect of three corrosion-resistant elements on corrosion resistance in concentrated hydrochloric acid. *Corros. Sci.* **43,** 171 (2001).
26. S.J. Pang, C.H. Shek, T. Zhang, K. Asami, and A. Inoue: Corrosion behavior of glassy $Ni_{55}Co_5Nb_{20}Ti_{10}Zr_{10}$ alloy in 1 N HCl solution studied by potentiostatic polarization and XPS. *Corros. Sci.* **48,** 625 (2006).
27. C.L. Qin, J.J. Oak, N. Ohtsu, K. Asami, and A. Inoue: XPS study on the surface films of a newly designed Ni-free Ti-based bulk metallic glass. *Acta Mater.* **55,** 2057 (2007).